Physica B: Condensed Matter 570 (2019) 320–323

Contents lists available at ScienceDirect

Physica B: Condensed Matter

journal homepage: www.elsevier.com/locate/physb

Metal-insulator phase diagram of the half-filled Anderson-Hubbard model

Anh-Tuan Hoang[a,b,*], Thi-Hai-Yen Nguyen[a], Duc-Anh Le[c]

[a] Institute of Physics, Vietnam Academy of Science and Technology, Viet Nam
[b] Graduate University of Science and Technology, Vietnam Academy of Science and Technology, Viet Nam
[c] Faculty of Physics, Hanoi National University of Education, Xuan Thuy 136, Cau Giay, Hanoi, 10000, Viet Nam

ARTICLE INFO

Keywords:
Metal-insulator transitions
Anderson-Hubbard model
Typical medium theory
Box and Gaussian disorder distributions

ABSTRACT

The metal-insulator phase transition diagrams of the Anderson - Hubbard model at half filling with the box and the Gaussian disorder distributions are obtained via typical-medium theory within an approximation to the equation of motion. The equations determining the boundary between the correlated metal, Mott insulator, and Anderson localization phases are derived. Our results are in good agreement with those found by the more sophisticated methods and indicate that on a qualitative level they do not depend on the choice of the above disorder distributions.

1. Introduction

The electronic interaction and randomness play an important role in determination for the properties of solids [1,2]. In particular, Coulomb interaction prevailing in strongly correlated electron systems and disorder which always exists in real materials are two main sources leading to metal - insulator transitions (MITs). When the latter is induced by the electronic correlation, it is referred to the Mott-Hubbard transition that can be described by the famous Hubbard model (HM). Nevertheless, a localization of the non-interacting particle due to random scattering induces an Anderson MIT when strong disorder prevents the diffusion of particles [3]. Furthermore, when both disorder and interactions are present their interplay could lead to many interestingly novel effects, which are challenging both theory and experiment in condensed matter physics as well as in the field of ultracold atoms loaded in optical lattices [4,5].

The dynamical mean field theory (DMFT) is a very successful method to capture the physics of the Mott - Hubbard MIT as well as strongly correlated materials. The essence of theory is the mapping of the lattice model onto a single impurity Anderson model (SIAM). The latter describes a single correlated impurity embedded in a bath of free electrons. The most challenging part is to solve the effective impurity model [6]. However, the arithmetical average of the local density of states (LDOS) obtained within such mean field theory is a failure to distinguish the extended states from the localized ones, so it is not suited to reveal the nature of Anderson localization. In order to get rid of this limitation, Dobrosavljevic and Kotliar have proposed the so-called statistical DMFT that includes a fully stochastic disorder fluctuations in space [7]. This theory well describes both Mott and Anderson-Mott transitions [8], however it requires extensive numerical computations.

Based on the geometrical average to the most probable value of the LDOS, the typical medium theory (TMT) has been developed to study systems with disorders by Dobrosavljevic and coworkers. Instead of the arithmetically averaged LDOS, the typical density of states (TDOS) is approximated by taking the geometrical averaging over all possible disorder configurations [9]. The TDOS is used as an order parameter for Anderson localization transition because the TDOS vanishes at a critical disorder strength. The TDOS can be easily calculated within the DMFT because it requires only one-particle quantities [10–12]. A reasonably accurate metal-insulator phase diagram of the box-disordered Anderson - Hubbard model at half-filling has been investigated within the TMT - DMFT using with different impurity solvers, such as the numerical renormalization group (NRG) method [10], the four boson technique (SB4) [11]. On the other hand, the ground state phase diagram of the half-filled Hubbard model with the Gaussian disorder distribution has been obtained by using other methods, such as an unrestricted Hartree -Fox approximation [13] and DMFT + Σ approach [14]. Therefore, it is difficult to compare the influence of the different distributions (the box and Gaussian) on the obtained phase diagrams, because we cannot know which of the findings are due to the disorder distribution and which ones are due to the approximate method being used.

In this report, the nonmagnetic ground state phase diagram of the HM at half-filling with the box and Gaussian disorder distributions is numerically constructed using the TMT - DMFT with an approximation to the equation of motion as an impurity solver. This approach allows

* Corresponding author. Institute of Physics, Vietnam Academy of Science and Technology, Viet Nam.
E-mail address: hatuan@iop.vast.ac.vn (A.-T. Hoang).

https://doi.org/10.1016/j.physb.2019.05.046
Received 26 April 2019; Received in revised form 24 May 2019; Accepted 28 May 2019
Available online 31 May 2019
0921-4526/

us to compare the effect of the different disorder distributions (the box and Gaussian) on the obtained averaged local densities of states as well as their phase diagrams.

2. Model and methods

We consider the system described by the Anderson- Hubbard model

$$H = -t \sum_{<ij>\sigma} (a_{i\sigma}^{\dagger} a_{j\sigma} + \text{H. c.}) + \sum_{i\sigma} \varepsilon_i n_{i\sigma} + U \sum_i n_{i\uparrow} n_{i\downarrow}, \tag{1}$$

where $a_{i\sigma}(a_{i\sigma}^{\dagger})$ denotes the annihilation (creation) operator of an electron with spin σ at site i, $n_{i\sigma} = a_{i\sigma}^{\dagger} a_{i\sigma}$ is the local electron number operator. t is the hopping amplitude for nearest neighbor sites i and j, and U is the on-site Coulomb repulsion. The local ionic energies ε_i follow a continuous probability distribution $P(\varepsilon_i)$. In our paper we consider the box (Bo) and Gaussian (Ga) distributions which are given by:

$$P_{Bo}(\varepsilon_i) = \frac{1}{\Delta_{Bo}} \Theta(\Delta_{Bo}/2 - |\varepsilon_i|), \tag{2}$$

$$P_{Ga}(\varepsilon_i) = \sqrt{\frac{6}{\pi \Delta_{Ga}^2}} \exp(-6\varepsilon_i^2/\Delta_{Ga}^2), \tag{3}$$

where Θ is the Heaviside step function and Δ denotes the disorder strength. In order to be able to compare the two different distributions, the value of Δ_{Ga} is chosen such that the variance of the Gaussian distribution equal that of the box distribution: $\Delta_{Bo} = \Delta_{Ga} = \Delta$.

The effective single-impurity Anderson Hamiltonian with different ε_i reads

$$H_{imp} = \sum_{\sigma} (\varepsilon_i - \mu) n_{i\sigma} + U n_{i\uparrow} n_{i\downarrow} + \sum_{k\sigma} \varepsilon_k c_{k\sigma}^{+} c_{k\sigma} + \sum_{k\sigma} (V_k c_{k\sigma}^{+} a_{i\sigma} + V_k^{*} a_{i\sigma}^{+} c_{k\sigma}). \tag{4}$$

Here μ is the chemical potential, $c_{k\sigma}$ $(c_{k\sigma}^{+})$ denotes the annihilation (creation) operator of the bath electrons with spin σ. The hybridization function is related to the matrix element V_k and the dispersion parameter ε_k by

$$\eta(\omega) = \sum_k \frac{|V_k|^2}{\omega - \varepsilon_k}. \tag{5}$$

For each ionic energy ε_i, we first calculate the local density of states (LDOS) $\rho(\omega, \varepsilon_i) = -\Im G(\omega, \varepsilon_i)/\pi$. We can then obtain the geometrically averaged LDOS $\rho_{geom}(\omega) = \exp[< \ln \rho(\omega, \varepsilon_i) >]$ as well as the arithmetically averaged LDOS $\rho_{arith}(\omega) = < \rho(\omega, \varepsilon_i) >$, where $< O(\varepsilon_i) > = \int d\varepsilon_i P(\varepsilon_i) O(\varepsilon_i)$ is an arithmetic mean of $O(\varepsilon_i)$. The lattice Green function is obtained by the Hilbert transformation

$$G(\omega) = \int d\omega' \frac{\rho_{\alpha}(\omega')}{\omega - \omega'}, \tag{6}$$

where α stands for either "geom" or "arith."

We consider the Bethe lattice with infinite connectivity, $\rho_0(\varepsilon) = 4\sqrt{1 - 4(\varepsilon/W)^2}/(\pi W)$, for which the self-consistent condition is given by

$$\eta(\omega) = W^2 G(\omega)/16. \tag{7}$$

In order to solve the effective single-impurity Anderson model (4) we will now employ the equations of motion method [6,15]. We focus on the paramagnetic case at half-filling, for which $< n_i \uparrow > = < n_i \downarrow > = < n_i > /2$ and $\mu = U/2$. The impurity Green function can be approximately obtained by equation

$$G(\omega, \varepsilon_i) = \frac{1 - < n_i > /2}{\omega - \varepsilon_i + U/2 - \eta(\omega) + U\eta(\omega)[\omega - \varepsilon_i - U/2 - 3\eta(\omega)]^{-1}} + \frac{< n_i > /2}{\omega - \varepsilon_i - U/2 - \eta(\omega) - U\eta(\omega)[\omega - \varepsilon_i + U/2 - 3\eta(\omega)]^{-1}}. \tag{8}$$

The equation (8) is exact in the non-interacting limit $U = 0$ [16]. In the non-disorder limit, $U \neq 0$, $\varepsilon_i = 0$, Eq. (8) is reduced to the (full) Hubbard III approximation of the Hubbard model at half-filling [17].

One has to solve Eqs. (6)–(8) numerically to get the averaged LDOS.

To proceed further, we note that in the half-filled band case, the ground state properties can be determined by the averaged LDOS at the Fermi level ($\omega = 0$): $\rho_{geom}(0) > 0$ denotes a metallic phase; $\rho_{arith}(0) = 0$ indicates a Mott insulator phase (hard gap); and $\rho_{geom}(0) = 0$, $\rho_{arith}(0) > 0$ denote an Anderson insulator phase (gapless). Due to a symmetry of $\rho_{\alpha}(\omega)$ and the spectral theorem, it is easy to prove that the Green function at the Fermi level is purely imaginary, $G(0) = -i\pi\rho_{\alpha}(0)$, then it is not difficult to find the averaged LDOS at the Fermi level from numerical solving Eqs. (7) - (8).

Next, we derive the linearized DMFT equations [18]. The purely imaginary of Green function at the Fermi level leads to the recursive relation $G(0)^{(n+1)} = -i\pi\rho_{\alpha}^{(n)}(0)$, where the left hand side in the $(n+1)$th iteration step is given by the result from the (n)th iteration step. On the metallic side the LDOS is arbitrarily small in the vicinity of the MIT region [18,19], therefore taking account of small $\rho_{\alpha}^{(n)}(0)$, by using Eq. (7) -(8) we get

$$\rho_{\alpha}^{(n+1)}(0, \varepsilon_i) = \frac{W^2}{16} \rho_{\alpha}^{(n)}(0) Z(\varepsilon_i), \tag{9}$$

where

$$Z(\varepsilon_i) = \frac{\varepsilon_i^2 + 3U^2/4 + 2\varepsilon_i U(1 - < n_i >)}{[\varepsilon_i^2 - U^2/4]^2}. \tag{10}$$

At the boundary between metal and insulator it yields $\rho_{\alpha}^{(n+1)}(0) = \rho_{\alpha}^{(n)}(0)$. Then, combining Eqs. (9) and (10) and evaluating the averaged on ε_i we get the equations determining the MIT for both geometrical and arithmetical means (W sets the energy unit):

$$1 = \frac{W^2}{16} \exp[I_{geom}(U, \Delta)], \tag{11}$$

where

$$I_{geom}(U, \Delta) = \int d\varepsilon_i P(\varepsilon_i) \ln Z(\varepsilon_i) \tag{12}$$

for the linearized DMFT with geometrical mean, and

$$1 = \frac{W^2}{16} I_{arith}(U, \Delta), \tag{13}$$

where

$$I_{arith}(U, \Delta) = \int d\varepsilon_i P(\varepsilon_i) Z(\varepsilon_i) \tag{14}$$

for the linearized DMFT with arithmetical mean. For simplicity of calculation, the atomic limit is adopted for $< n_i >$:

$$< n_i > = \begin{cases} 2, & \text{if } \varepsilon_i < -U/2, \\ 1, & \text{if } -U/2 < \varepsilon_i < U/2, \\ 0, & \text{if } \varepsilon_i > U/2. \end{cases} \tag{15}$$

Then for the Gaussian distribution the integrals (12) can be obtained numerically, while for the box distribution both integrals (12) and (14) are evaluated analytically with results

$$I_{geom}(U, \Delta) = 2 + \ln[3(U/2)^2 + (\Delta/2)^2] + \frac{2\sqrt{3}U}{\Delta} \arctan\left(\frac{\Delta}{\sqrt{3}U}\right) - 2\ln|(U/2)^2 - (\Delta/2)^2| - \frac{2U}{\Delta} \ln\frac{\Delta + U}{|\Delta - U|}, \quad \text{if } \Delta > U, \tag{16}$$

$$I_{geom}(U, \Delta) = -\frac{4U}{\Delta} \ln 2U + \left(1 + \frac{2U}{\Delta}\right) \ln\left[\left(\frac{\Delta}{2} + U/2\right)^2 - \frac{U^2}{4}\right] + \frac{U}{\Delta} \ln\frac{\Delta + 3U}{\Delta + U} + \frac{\pi U}{\sqrt{3}\Delta} + 2 - 2\ln|(U/2)^2 - (\Delta/2)^2| - \frac{2U}{\Delta} \ln\frac{\Delta + U}{|\Delta - U|}, \quad \text{if } \Delta < U. \tag{17}$$

The integral (14) converges if only $\Delta < U$ and in this case

$$I_{arith}(U, \Delta) = \frac{2}{(U/2)^2 - (\Delta/2)^2} + \frac{2}{\Delta U} \ln\frac{\Delta + U}{|\Delta - U|}. \tag{18}$$

We note that our preliminary linearized-DMFT result for the half filled Anderson - Hubbard model with the box disorder distribution has been reported in Ref. [15], where a rough approximation is used for <

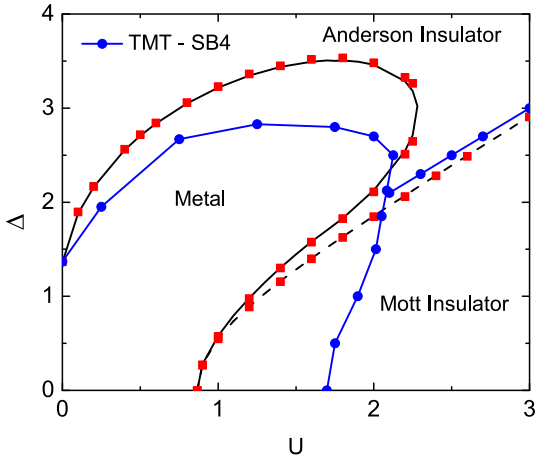

Fig. 1. T = 0 phase diagram for the half filled Anderson - Hubbard model with the box disorder distribution: a comparison between TMT-DMFT with the EOM and the SB4 result in Ref. [11] (solid line with dots). In our result: solid (dashed) lines are determined by using geometrical (arithmetical) averaging from the linearized DMFT; squares are obtained from numerical solution of the DMFT equations. Energy parameters U, Δ are in the unit set by $W = 1$.

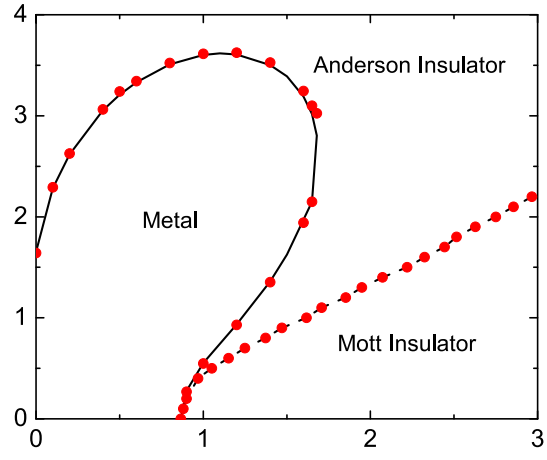

Fig. 2. T = 0 phase diagram for the half filled Anderson - Hubbard model with the Gaussian disorder distribution, obtained from TMT-DMFT with the EOM. Solid line is determined by using geometrical averaging from the linearized DMFT; dots are obtained from numerical solution of the DMFT equations, dashed line is a guide to the eye.

$n_i > : < n_i > \; = 1, \forall \varepsilon_i$.

3. Results and discussion

Now we turn to present our numerical results with $W = 1$ as the energy unit. At $T = 0$, the interaction - disorder ($U - \Delta$) phase diagram of the AHM with the box disorder distribution is shown in Fig. 1. We compare our result with result obtained from the numerical solution using four slave bosons to the TMT-DMFT [11], which is generally consistent with that found from TMT-DMFT with the NRG impurity solver [10] and from the statistical DMFT [8]. It is seen that the overall structure is reproduced: the two insulating phases, Mott insulator and Anderson localization, surround the correlated metal. The latter is identified for small values of U and Δ. Whereas, the Mott phase stabilizes with increasing U, and large Δ favors the Anderson localization. Furthermore, the shape of metallic region is in good agreement and the boundary between two types of insulators occurs at $\Delta \approx U$ when $U \geq 2$. In the non-interacting system, as in Refs. [13,14] our method predicts the Anderson localization to take place at a critical value $\Delta_c(U = 0) = e/2 \approx 1.36$. However, in our phase diagram the presence of disorder increases the critical value for the Mott-Hubbard MIT from $U_c(\Delta = 0) = \sqrt{3}/2$. This value is significant smaller than found from TMT-DMFT with the NRG and the SB4 [10,11] as well as from the statistical DMFT [8]. To sum up the comparison, our result is in fairly good agreement with known numerical results in Refs. [8,10,11], therefore the detection of localization within TMT-DMFT with the EOM is justified on a qualitative level. The ground state phase diagram of the AHM with the Gaussian disorder distribution is presented in Fig. 2. There is not a big difference between the two phase diagrams shown in Figs. 1 and 2. For both disorder distributions one finds a metallic core for small and intermediate strengths of both the disorder and the interaction. Also the re-entrance behavior as a function of Δ for intermediate U is similarly predicted for both disorder distributions. However, the results quantitatively differ each other. We find that for small values of U the critical disorder strength in the system with the Gaussian distribution is larger than those in the system with the box distribution. For example, in the non-interacting system the critical disorder ($\Delta_c(U = 0) \approx 1.66$) for the Gaussian distribution larger than those ($\Delta_c(U = 0) \approx 1.36$) for the box distribution, which is in reasonable agreement with numerical results from the literature [20]. Furthermore, for the Gaussian disorder distribution the direct metal - Mott insulator transition is found for weaker disorders Δ. In this case, the integral (14) is divergent for $\Delta \neq 0$, so the Mott insulator phase is determined only from numerical solution of the DMFT equations. From Fig. 2 one can see that the border between the Mott and the Anderson insulators for the system with the Gaussian distribution is located lower than those with the box distribution in the (U, Δ) plane. To illustrate these results we calculate the LDOS in the a band center ($\omega = 0$) as functions of disorder Δ at fixed $U = 0.5$ for both disorder distributions. As can be seen from Fig. 3, for small U ($U < \sqrt{3}/2$) while the geometrically averaged LDOS, i. e. the metallicity, decreases with increasing disorder strength and vanishes at the critical disorder strength, the arithmetically averaged LDOS is found to be equal the geometrically averaged LDOS at weak disorder but then it has a rather slow decrease and remains finite at critical one. In addition, the critical disorder strength for Gaussian distribution larger than those obtained for the box distribution. The behavior of $\rho_{geom}(0)$ for both disorder distributions at intermediate values of interaction ($\sqrt{3}/2 < U \leq 2.3$ for the box distribution and $\sqrt{3}/2 < U \leq 1.7$ for the Gaussian distribution) is shown in Fig. 4 ($U = 1.2$): when increasing Δ to critical value $\rho_{geom}(0)$ abrupt rises from zero, then gains its maximal value, after that decreases to zero again, i. e. in this case, when the disorder is increased at fixed U the MIT occurs twice, in which at the first one the disorder stabilizes the

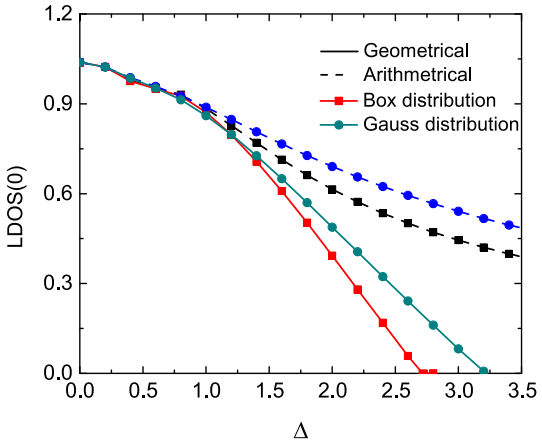

Fig. 3. Geometrically and arithmetically averaged local density of states in a band center ($\omega = 0$) at $U = 0.5$ as a function of Δ for the box and the Gaussian disorder distributions. Solid (dashed) lines are determined by using geometrical (arithmetical) averaging. Lines with squares (dots) are obtained for the box (the Gaussian) disorder distribution.

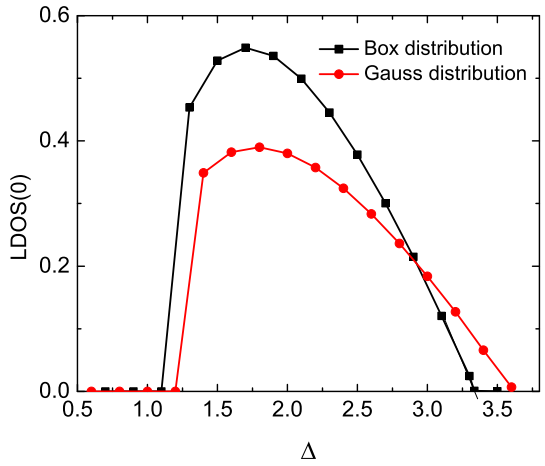

Fig. 4. Geometrically averaged local density of states in a band center ($\omega = 0$) at $U = 1.2$ as a function of Δ for the box and the Gaussian disorder distributions. Lines with squares (dots) are obtained for the box (the Gaussian) disorder distribution.

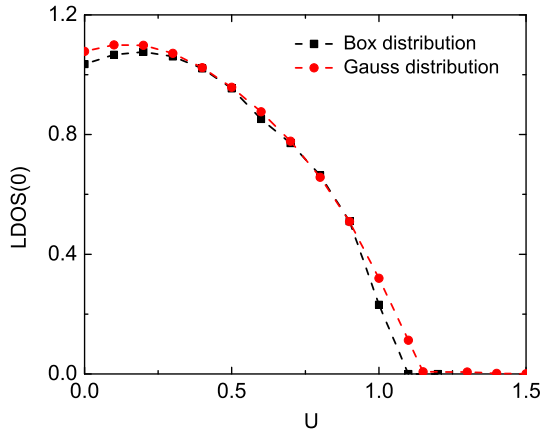

Fig. 5. Arithmetically averaged local density of states in a band center ($\omega = 0$) at $\Delta = 0.6$ as a function of U for the box and the Gaussian disorder distributions. Lines with squares (dots) are obtained for the box (the Gaussian) disorder distribution.

metallic phase. We have also plotted the arithmetically averaged LDOS $\rho_{arith}(0)$ as a function of interaction U at fixed $\Delta = 0.6$ for both disorder distributions in Fig. 5. The two curves have the same behavior and a little difference between them is found only for weak and strong interactions with the larger critical interaction strength for the Gaussian distribution. We assume the higher disorders associated with the exponential nature of the Gaussian distribution are responsible for quantitative differences between the box and the Gaussian distribution results.

It is worth to compare our TMT-DMFT phase diagram with the Gaussian disorder distribution with those obtained by using other methods. In Ref. [14] the phase diagram of nonmagnetic Anderson-Hubbard model at zero temperature with the same bare semi-elliptic DOS was presented. The DMFT approach was used, but note that the self-energy was not obtained by geometrically averaging over different disorder realization. In fact, the authors of Ref. [14] used a disorder-averaged self-energy contribution that completely misses correlations between disorder interaction contributions. Consequently, the Anderson MIT critical disorder $\Delta(U)$ is independent on interaction U. Also, the main difference is that our data indicate the movement of one type of insulator to the other without crossing the metallic phase occurs at much lower disorder than in Ref. [14], keeping in mind that the variance of the Gaussian distribution equal Δ^2 in Ref. [14]. Next, we compare our phase diagram with those for a Gaussian site-disordered Anderson -Hubbard model on a simple cubic lattice at half-filling calculated by using an unrestricted Hartree-Fock approximation in Ref. [13]. The qualitative agreement is surprisingly good. In particular, in both phase diagram the direct metal- Mott insulator transition is clearly limited to a small region of the (U, Δ) plane, where both interaction and disorder are weak.

4. Conclusions

In summary, in this paper the nonmagnetic ground state phase diagram for the box and the Gaussian site-disordered Anderson-Hubbard model at half-filling are obtained within the typical-medium theory using the equation of motion as an impurity solver. Our obtained result for the box disorder distribution is consistent with those found from the statistical DMFT and the TMT-DMFT with the NRG and the SB4. This supports that the statistical DMFT and the TMT - DMFT lead to qualitatively agreeing result in general. Our phase diagram for the Gaussian disorder distribution is in good agreement with those obtained by using unrestricted Hartree-Fock approximation in Ref. [13] and overcomes main shortcoming of the phase diagram in Ref. [14]. The similar overall form of the phase diagram as well as the averaged local densities of states obtained from the box and Gaussian disorder distribution indicate that qualitatively they are not dependent on the choice of the above disorder distributions. However, note that this conclusion is derived within the TMT - DMFT with an approximation to the equation of motion as an impurity solver.

An important advantage of our approach is the considerable smaller computational effort, which enable the use for a more complex (and realistic) system. These may be the subject of our future study.

Conflicts of interest

No conflict of interest.

Acknowledgments

This research is funded by National Foundation for Science and Technology Development (NAFOSTED) under Grant No. 103.01-2017.56.

References

[1] P.A. Lee, T.V. Ramakrishnan, Rev. Mod. Phys. 57 (1985) 287.
[2] D. Belitz, T.R. Kirkpartrick, Rev. Mod. Phys. 66 (1994) 261.
[3] P.W. Anderson, Phys. Rev. 109 (1958) 1492.
[4] K. Byczuk, W. Hofstetter, D. Vollhardt, Int. J. Mod. Phys. B 24 (2010) 1727.
[5] S.S. Kondov, et al., Phys. Rev. Lett. 114 (2015) 083002.
[6] A. Georges, et al., Rev. Mod. Phys. 68 (1996) 13.
[7] V. Dobrosavljevic, G. Kotliar, Phys. Rev. Lett. 78 (1997) 3943.
[8] D. Semmler, et al., Phys. Rev. B 84 (2011) 115113.
[9] V. Dobrosavljevic, A.A. Pastor, B.K. Nikolic, Europhys. Lett. 62 (2003) 76.
[10] K. Byczuk, W. Hofstetter, D. Vollhardt, Phys. Rev. Lett. 94 (2005) 0564021.
[11] M.C.O. Aguiar, V. Dobrosavljevic, E. Abrahams, G. Kotliar, Phys. Rev. Lett. 102 (2009) 156402.
[12] R.D.B. Carvalho, M.A. Gusmao, Phys. Rev. B 87 (2013) 085122.
[13] M.A. Tusch, D.E. Logan, Phys. Rev. B 48 (1993) 14843.
[14] E.Z. Kuchinskii, I.A. Nekrasov, M.V. Sadovskii, J. Exp. Theor. Phys. Lett. 106 (2008) 581.
[15] A.T. Hoang, T.H.Y. Nguyen, Commun. Phys. 28 (2018) 163.
[16] V. Dobrosavljevic, Int. J. Mod. Phys. B 24 (2010) 1680.
[17] J. Hubbard, Proc. Roy. Soc. Lond. A 281 (1964) 401.
[18] R. Bulla, M. Potthoff, Eur. Phys. J. B. 13 (2000) 257.
[19] K. Byczuk, Phys. Rev. B 71 (2005) 205105.
[20] E. Ekuma, C. Moore, H. Terletska, et al., Phys. Rev. B 92 (2015) 014209.